



Pig adipose tissue of two different breeds and locations: morphology and Raman studies

Viktoriya A. Pchelkina* , Irina M. Chernukha ,
Marina A. Nikitina , Nikolai A. Ilin

V.M. Gorbатов Federal Research Center for Food Systems of RAS, Moscow, Russia

* e-mail: v.pchelkina@fncps.ru

Received 25.08.2022; Revised 14.09.2022; Accepted 04.10.2022; Published online 17.10.2022

Abstract:

According to the recent data, there are 4–5-local pig breeds left in Russia by now. Livni is among them. This breed is characterized by high fat content. Back fat has been analyzed earlier. We aimed to assess fat morphometrics from other localizations in pigs.

Sacral, axillary, and perirenal fat samples from 6-month-old Duroc and Livni pig breeds were analyzed using morphological and Raman-based techniques.

Livni adipocytes were characterized by dense packing with a polyhedron-like structure. In Duroc fat, they were more rounded (spherical). A “two-phase” cell disperse was identified in all samples. Fat cells in Livni pigs were bigger than those in the Duroc breed: 70–102, 15–18, and 26% for sacral, axillary, and perirenal locations. Differences in the intensity of the Raman signal between the samples were found: in the samples of subcutaneous adipose tissue, more intense peaks were observed, which are responsible for unsaturation; the samples of Livni axillary fat were characterized by greater unsaturation than sacral fat.

Livni and Duroc adipocytes differ from each other in form and size and the difference depends on location. Pork fat from local breeds is expected to have potentially more health protecting (for animals) and health promoting (for consumers) properties.

Keywords: Fat, pigs, Duroc, Livni, histology, adipocytes, morphometry, Raman spectroscopy

Funding: This work was financially supported by the Russian Science Foundation (RSF) (project No. 21-76-20032).

Please cite this article in press as: Pchelkina VA, Chernukha IM, Nikitina MA, Ilin NA. Pig adipose tissue of two different breeds and locations: morphology and Raman studies. *Foods and Raw Materials*. 2023;11(1):1–9. <https://doi.org/10.21603/2308-4057-2023-1-547>

INTRODUCTION

Worldwide, there are around 950–960 million pigs (according to various sources), of which 80% are in Asia and Europe. The domestic pig (*Sus scrofa*) was domesticated in China and Europe about 9000 years ago, and there are now about 350 breeds [1, 2].

In the USSR, the number of pigs in 1980 exceeded 70 million and 22 local breeds were registered, including the Ukrainian Steppe White, Siberian Northern, Livni, Kemerovo, Mirgorod, Urdjum, Semirechensk, etc., which accounted for one third of the total number of livestock. Although pigs in Russia were descended from imported breeds, they were subsequently adapted to local conditions, and breeds with unique characteristics were developed. Before the beginning of the 20th century, the number of livestock totalled about 20 million [3].

The crisis of the 1990s led to a reduction in the number of livestock to 13 million [4]. There has been a significant growth in pig breeding since 2010 as a result of the state sectorial target programme “Development of pig breeding in the Russian Federation for 2010–2012”, approved by Order № 567 of the Ministry of Agriculture of Russia of 30 November 2009. Since then, pig farming in Russia has been gaining momentum: between 2016 and 2020, the number of pigs increased from 23.3 to 26.9 million.

Modern pig production is based on the hybridisation of three pure breeds: Yorkshire or Large White, Landrace, and Duroc [5]. In Russia, the reduction in the number of local breeds is due to the global trend towards the industrial use of imported cosmopolitan breeds as they are well adapted to intensive production systems [6].

Local breeds, which have unique variability, are deemed, together with their wild relatives, a valuable genetic resource. They are characterized by greater individual variability, strength of constitution, greater stress and weather resistance, and the highest quality meat [6–9]. However, they have a lower growth potential and protein deposition [10].

As of the beginning of 2021, the pig breeding stock in Russia is represented by eight breeds of pigs, including the Large White (53.4%), Yorkshire (21.4%), Landrace (18.9%), and Duroc (5.2%). Other domestic breeds account for 0.8% of the stock [11].

All species of the *Suidae* (swine/pigs) family have well-developed subcutaneous as well as visceral adipose tissue, but their structure has very specific features due to both genetic and paratypical factors. One of the main objectives of the continuous improvement of pork production is to regulate the amount of fat.

All pig breeds can be divided into three groups according to lean meat yield per carcass: bacon – above 58% (Urdjum, Latvian White, Hampshire, Estonian Bacon); lard – less than 50% (Large Black, Breitovo, Berkshire, Mangalica) and universal, which occupy an intermediate position (Polish-Chinese, Lithuanian White, Kemerovo, Ukrainian Steppe White, North Caucasian, Livni) [12].

It should be noted that domestic breeds are characterised by a significant proportion of stored fat on the carcass, relatively low early maturity and associated low feed conversion ratio. This is also seen as an advantage for meat products from foreign breeds. There are also differences in fat quality; for example, the back fat of Irish-bred pigs is more malleable than that of domestic pigs, due to the ratio of saturated/unsaturated fatty acids, which in turn affects the stress tolerance of the animals [13].

Adipose tissue is the largest and most dynamic energy reservoir – most energy is stored as triglycerides in fat cells (adipocytes), and also an active metabolic and endocrine organ that secretes several bioactive peptides (adipokines). There are four fat depots with varying anatomical locations: visceral, subcutaneous, intermuscular, and intramuscular [14, 15]. Each fat depot has specific morphological and metabolic properties [16].

Morphological studies of (mainly) back fat of pigs of different breeds have been conducted by several authors [17–19]. However, there is very little information on adipose tissue in other locations. Lard and universal breeds generally have larger adipose tissue cells than bacon pigs of the same body weight. For example, Meishan lard pigs have larger back fat adipocytes than Landrace bacon pigs [19]. In addition, local pig breeds are characterized by an earlier maturation (development) of adipose tissue [20].

Breed is also known to have a direct impact on the quality and fatty acid composition of adipose tissue [21]. Significant anatomical differences in fatty acid composition in pigs have been reported [16]. Raman spectroscopy is a proven method for determining the

concentration of major fatty acid groups [22]. The use of Raman spectroscopy for fat estimation has a significant practical advantage as it does not require complex extraction or purification processes and can be used both for rapid screening to control fat quality and for fundamental research into the factors affecting its polymorphic transitions and stability.

This means that it is imperative that the adipose tissue of pigs of different breeds and different locations is studied, as this will provide an understanding of the potential of lipogenesis and allow us to assess the quality of these adipose tissues as a valuable raw material for the meat industry, especially in pigs with varying degrees of body fat. In this regard, the aim of the study was to investigate and compare the morphological features of adipose tissue of different locations in pigs of two breeds with different productivity levels: Duroc (bacon) and Livni (universal).

STUDY SUBJECTS AND METHODS

In our experiment, we analyzed 6-month-old pigs of two breeds, namely Livni ($n = 6$, private farm, Livensky district, Orel region) and Duroc ($n = 8$, LLC Breeding-Hybrid Center, Voronezh, under the conditions of the experimental farm of the L.K. Ernst Federal Science Center for Animal Husbandry). The following subcutaneous (fat) and internal adipose tissue samples were taken from the pigs: sacral fat, subcutaneous axillary, and internal perirenal.

The thickness of the subcutaneous fat was measured with a flexible ruler, accurate to 0.5 mm.

Morphological (histological) examination. To study adipose tissue morphology, the samples were preserved in a 10% neutral buffered formalin solution for 72 h at room temperature. Then a $1.5 \times 1.5 \times 0.5$ cm slice was taken from each sample, washed with cold running water for 4 h and compacted in gelatin at an ascending concentration (12.5 and 25%) (AppliChem GMBH, Germany) at 37°C for 8 h each using a thermostat (SPU, Russia). 14- μm thick sections were prepared on a MIKROM-HM525 cryostat (Thermo Scientific, USA). The obtained sections were placed on Menzel Glaser slides (Thermo Scientific, USA) and stained with Erlich haematoxylin and a 1% aqueous-alcoholic eosin solution (BioVitrum, Russia) according to conventional methods [23]. The sections were encased in glycerol-gelatin. The histological preparations were studied and photographed using an AxioImager A1 light microscope (Carl Zeiss, Germany) and an AxioCam MRc 5 video camera (Carl Zeiss, Germany).

To calculate the area of adipocytes, 14 μm -thick sections were obtained from formalin-fixed samples, placed on slides, embedded in a drop of a saline solution, and immediately examined using the AxioVision 4.7.1.0 image analysis system (Carl Zeiss, Germany) (modified technique) [24]. At least three slices were made for each specimen. The adipocyte area was measured interactively with an accuracy of $\pm 1.0 \mu\text{m}^2$.

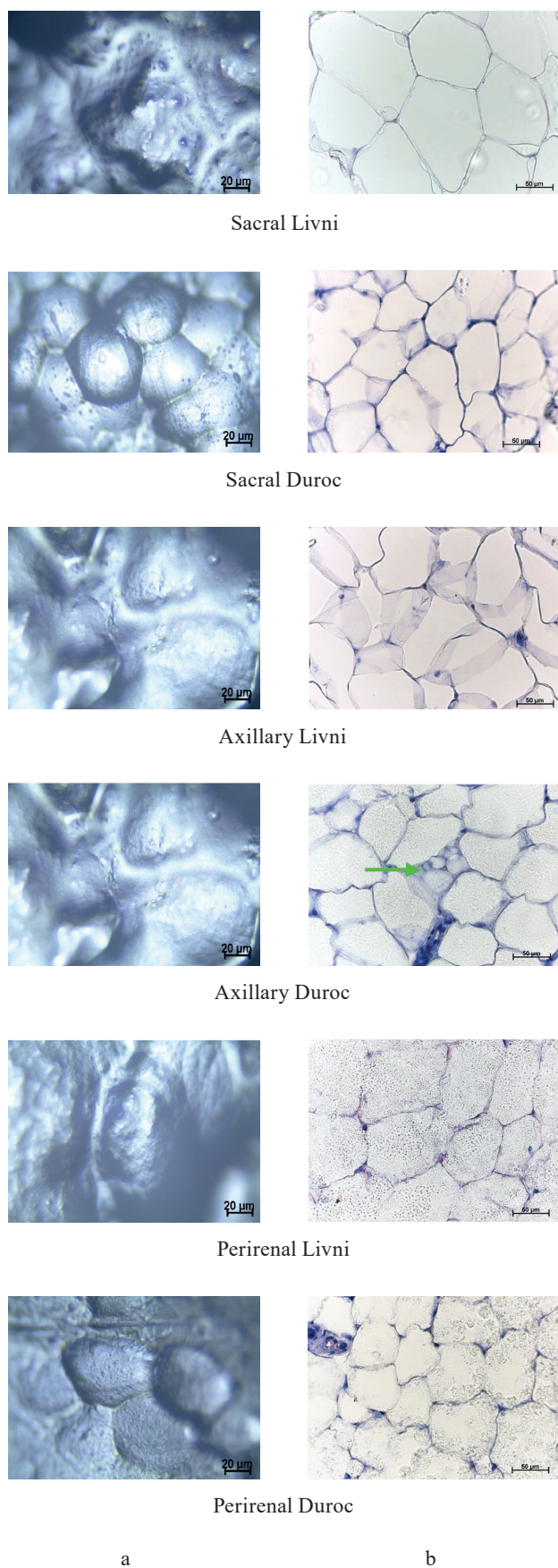


Figure 1 Representative photographs of adipose tissue samples from Livni and Duroc pigs: (a) structure without staining (20×); (b) hematoxylin and eosin staining (40×). The arrow shows a beige adipocyte

For subcutaneous adipose tissue samples, cell areas of the outer (just under the skin) and inner (closer to the muscle) layers were counted of at least 100 for each layer.

Raman spectroscopy. Raman spectroscopy was used to evaluate the total fatty acid profile of the studied samples [22, 25]. The spectra were collected on a Renishaw model inVia Reflex confocal Raman dispersive spectrometer (Renishaw plc, Wotton-under-Edge, UK) using a 785-nm laser. The spectrometer was calibrated by recording the Raman spectrum of a silicon crystal wafer at 520 cm^{-1} (exposure time 1 s, laser power 10 mW, 1 scan). Raman spectra were obtained directly from the fat samples by placing them under the spectrometer’s microscope, an L50× magnification was used to focus the laser on the surface of the samples. The laser power was 100 mW, exposure time 10 s, 3 scans (accumulations). Measurements were recorded in the detection range of $700\text{--}1800\text{ cm}^{-1}$. The laser power and integration time were carefully optimized to avoid the photodegradation of fat samples. An average of six spectra was used for each sample.

The raw Raman spectra included noise, fluorescence background, and spectral overlap of adjacent bands, making them difficult to identify visually. The entire spectral analysis and pre-processing was performed using Renishaw WiRE 5.2 software (Renishaw plc, Wotton-under-Edge, UK). Pre-processing included cosmic ray removal, baseline correction using intelligent polynomial algorithms, smoothing using the Savitzky-Golay algorithm, and normalization.

Statistical processing of the results. Statistical analysis of the data was performed using the STATISTICA software package, version 10.0 (StatSoft, Inc., USA). The results were presented as a mean (Mean), standard error of the mean (\pm SE), minimum and maximum [MIN MAX] interquartile range (R 25/75). The geometric mean (GeoMean) was used to analyze the spectral intensities. The differences were considered to be significant and the association between the indicators was considered to be at a level of probability not more than 0.05.

Correlation matrices (correlation matrices in the form of square tables, with row and column headings representing the variables to be processed, and the intersection of the rows and columns displaying the correlation coefficients for the corresponding pair of features) were generated in the RStudio IDE using the R programming language with the *psych* function. The raw data in *.xls format was converted to csv format (comma delimiters). The libraries ggplot2, tidyverse, ggthemes, RColorBrewer, grid, and gridExtra were used for data visualization. A scatter plot, representing the values of two variables as points on the Cartesian plane, was also obtained.

RESULTS AND DISCUSSION

On visual inspection, the fat samples had a white to pale pink colour and soft consistency, and were odorless. The average thickness of the subcutaneous fat samples

Table 1 Results of the morphometric analysis of adipose tissue samples of different locations

Locus	Layer	Adipocyte area, μm^2 (Mean \pm SE [MIN MAX])	
		Livni	Duroc
Sacral	External	7063.29 \pm 166.66 [3928.44–2107.29]	4139.92 \pm 49.68 [2605.71–6022.94]
	Internal	9432.96 \pm 152.47 [5725.98–14255.27]	4677.37 \pm 63.74 [2851.51–6761.85]
Axillary	External	4172.14 \pm 61.48 [1550.5–6684.84]	3534.79 \pm 50.53 [2579.32–4522.09]
	Internal	5404.43 \pm 74.35 [3419.95–10012.89]	4691.24 \pm 77.99 [3304.18–6188.9]
Perirenal		5328.14 \pm 64.33 [2931.98–8825.86]	4215.01 \pm 23.15 [2884.72–313.18]

was: sacral Livni – 39.8 ± 1.6 mm; sacral Duroc – 16.70 ± 0.47 mm; axillary Livni – 8.80 ± 0.37 mm; and axillary Duroc – 5.5 ± 0.5 mm.

Microstructure analysis revealed that in the subcutaneous fat samples (sacral and axillary), adipocytes were presented as polygonal cells, with slightly rounded edges. The adipocytes of Livni pigs were tightly packed in the shape of a polyhedron, while in Duroc pigs the cells were more rounded (spherical) in shape. A large fat droplet was located in the central part of the cells, displacing the oval nucleus to the periphery of the cell. Thin and sparse collagen fibres were located between the cells in Livni pigs, while in Duroc pigs thicker intercellular layers of connective tissue with frequent collagen fibres were present. This structure is characteristic of mature white adipocytes. The adipocytes of internal body fat (perirenal) in both breeds differed in their more rounded shape (Fig. 1).

In the axillary adipose tissue samples from Duroc pigs, single adipocytes were found to be polygonal in shape and smaller in size, having a rounded nucleus closer to the centre of the cell and several fat droplets of different sizes (from 3 to 20 μm in diameter). This cell structure is characteristic of beige adipocytes [26]. The presence of beige adipocytes in pig adipose tissue has been described, for example, by Zhao *et al.* and is of interest in terms of evaluating the therapeutic and prophylactic potential of pig fat [27]. No such cells were detected in samples from other locations or in all samples from Livni pigs.

The results of the morphometric analysis of adipose tissue cells of different locations from Duroc and Livni pigs are shown in Table 1. Adipose tissue growth is known to result from hypertrophy (increased size of adipocytes) and hyperplasia (increased number of adipocytes) [14]. Adipocytes increase in number and size with increasing weight and age of animals, which affects the thickness of the fat. Early in life, adipose tissue in pigs grows mainly through hyperplasia, and after a significant increase in cell number, adipocytes begin to hypertrophy through triglyceride accumulation. A biphasic distribution of adipose cells into small and large cells was observed in all adipose tissue samples, which is consistent with the results of other studies. According to [19], small backfat adipocytes accounted for 15–19% of the total population in 5-month-old Meishan and Landrace pigs. In our study, the proportion of small adipocytes was 8% in the sacral Livni samples,

11% in the sacral Duroc samples, 8% in the axillary Livni samples, 14% in the axillary Duroc samples, 9% in the perirenal Livni samples, and 10% in the perirenal Duroc samples.

Correlation matrices of fat cells are shown in Fig. 2. Above the main diagonal are correlation coefficients for the area of adipocytes of different locations. Below the main diagonal is a visualization of the correlation between fat cells of different locations. The main diagonal contains cell density distribution diagrams. According to the data obtained, the area of adipocytes in the external and inner layers of subcutaneous fat correlated well with each other: the correlation coefficient was 0.86 for the sacral Livni samples, 0.75 for the axillary Livni samples, 0.75 for the sacral Duroc samples, and 0.95 for the axillary Duroc samples. On the contrary, there is no linear correlation between the adipocytes of perirenal and other locations on carcasses of Livni breed pigs, unlike pigs of the Duroc breed.

Figure 3 presents a dot plot of fat cell dispersion as a function of area. Along the main diagonal, there are fat cells of various locations (sacral, axillary, and perirenal), below is a visualization of the adipocytes of the Livni (green dots) and Duroc (red dots) breeds using a scatter diagram, while the correlation coefficients are at the top of the main diagonal. The difference in cell area distribution between the breeds and locations is clearly visible. However, the correlation is low between inner perirenal and axillary fat, and the dots are chaotically arranged and not clustered in the diagram.

The results of the morphological study showed that there were differences in the cellular structure between the adipose tissue of pigs of different breeds, which is consistent with the published works of other authors [17, 24]. In our study, the adipocytes of fat samples from Livni pigs were the largest compared with samples from the Duroc breed: the cell area in the sacral Livni samples exceeded that of sacral Duroc adipocytes by an average of 70 and 102% ($p \leq 0.01$), in the axillary Livni samples by 18 and 15% for the external and internal layers respectively; and in the perirenal Livni samples by 26%.

The adipocyte area of subcutaneous fat was found to differ as a function of its location on the animal's body – larger cells were detected in the samples of the sacral fat of both breeds compared to the axillary samples. At the same time, there were larger adipocytes in the internal layers of the fat than in the external layers: for sacral

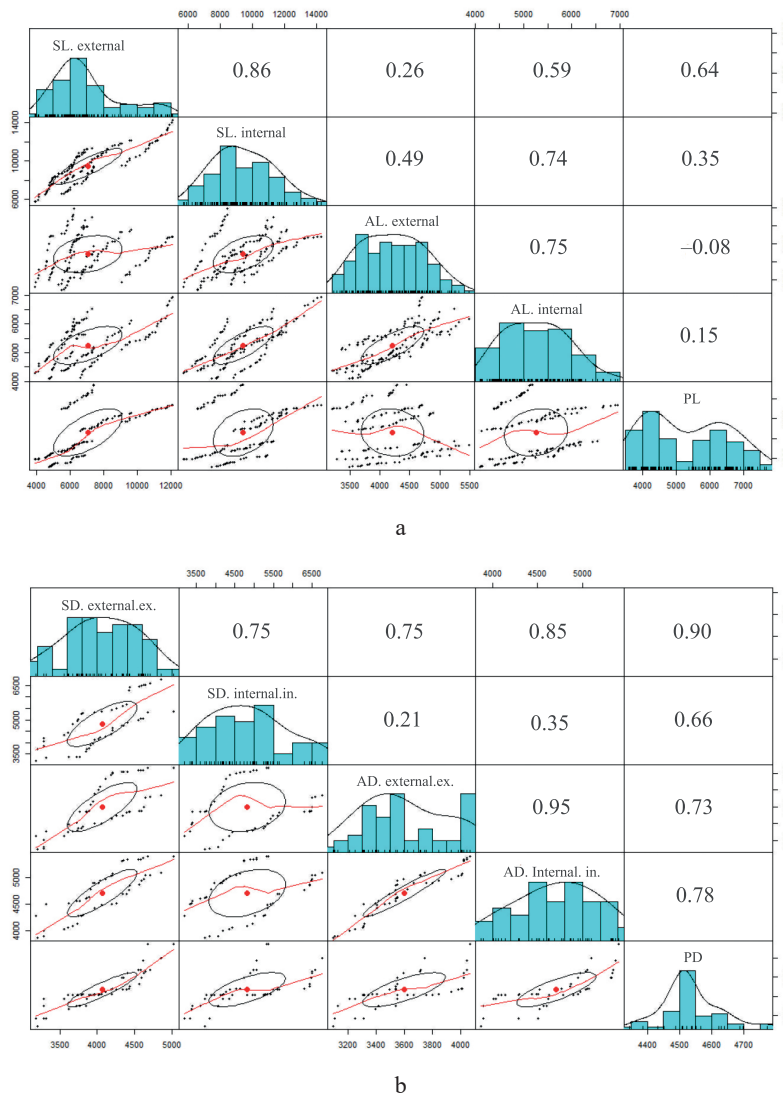


Figure 2 Correlation matrices of fat cells of various locations: (a) for the Livni breed; (b) for the Duroc breed

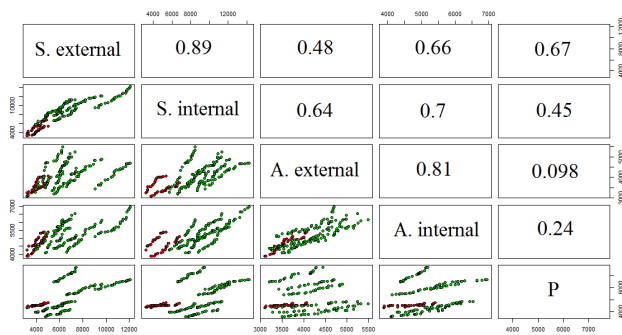


Figure 3 Scatter diagram and correlation coefficients of fat cells of various locations of the Livni (green dots) and Duroc (red dots) breeds. S, A, and P are acral, axillary, and perirenal fat, respectively

Livni by 33.5%; for sacral Duroc by 13%; for axillary Livni by 29.5%; and for axillary Duroc by 32.7%. The large size of adipocytes likely contributes to a greater increase in sacral fat thickness in Livni pigs compared

to Duroc pigs. This means that pigs of the Livni breed were characterised by a higher development of adipose tissue at all loci.

The Raman spectra of lipids are mainly represented by bands due to oscillations of hydrocarbon chains (saturated and unsaturated structures) [28, 36]. The Raman spectra of adipose tissue samples contain essentially the same signals (Fig. 4), whose characteristics are given in Table 2. Differences in Raman signal intensity were identified between the samples from the same breed but having different locations on the carcass and between pig breeds.

As the difference between individual fatty acids lies in the length of carbon chains and the number and arrangement of double bonds, they have similar Raman spectra [31, 32]. This means that the problem of overlapping peaks from different fatty acids arises when analyzing adipose tissue samples [33, 34]. To determine the relative content of unsaturated fatty acids in each sample, we calculated the ratio of the intensity

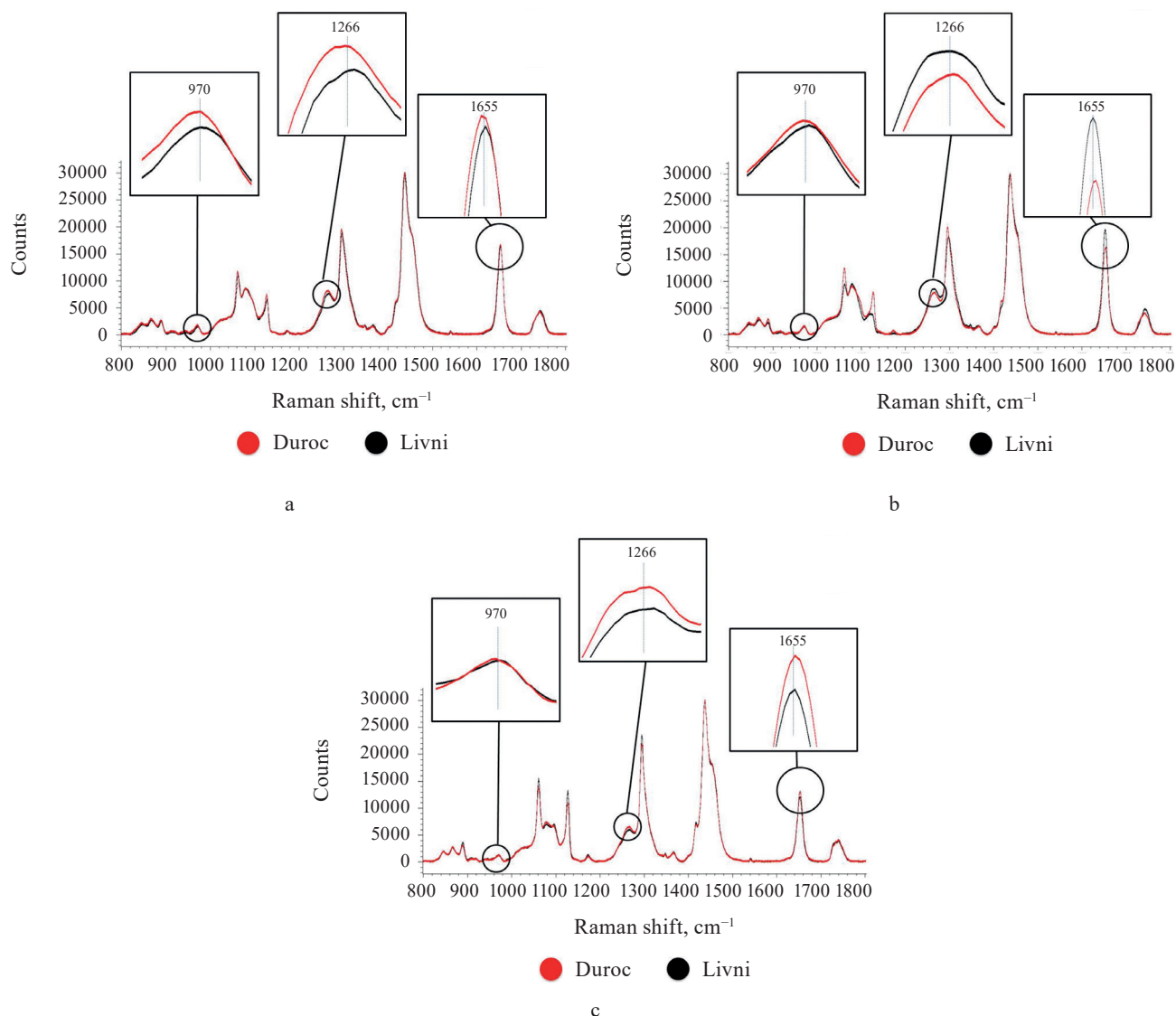


Figure 4 Raman spectra of adipose tissue samples: (a) sacral fat; (b) subcutaneous axillary; (c) internal perirenal

Table 2 Characteristics and intensity of obtained Raman spectra of adipose tissue signals from two breeds of pig

Band number	Band position, cm ⁻¹	Mode of vibration [25, 29]	Livni			Duroc		
			Sacral	Axillary	Perirenal	Sacral	Axillary	Perirenal
1	868	C-C stretching	2665.18	2771.44	2683.69	2881.81	3130.60	2694.85
2	970	=C-H out-of-plane bend <i>cis</i> isomer	1447.37	1535.33	1207.89	1771.12	1608.46	1227.42
3	1061/1068	C-C aliphatic out-of-phase stretching	10945.40	9692.98	15466.90	11711.90	12470.8	13913.00
4	1080	C-C aliphatic stretching	8056.34	9091.33	6927.31	7998.18	8474.42	7347.22
5	1127	C-C aliphatic in-phase stretching	6440.39	4301.32	13255.10	7408.41	7992.15	11057.00
6	1266/1 272	=C-H symmetric rock <i>cis</i> isomer	7440.65	8533.44	5761.50	7995.07	7695.84	6345.80
7	1297/1 301	CH ₂ twisting	19402.40	18106.70	23546.30	20242.40	20372.4	21913.2
8	1368	CH ₂ symmetric deformation (umbrella)	1670.61	1618.70	1736.24	1495.95	1532.85	1624.32
9	1430/1 460	CH ₂ symmetric deformation (scissoring)	30466.10	30569.60	29897.70	30510.40	30128.40	29999.60
10	1655	C=C stretching	16372.50	19602.30	12018.20	16667.70	16403.80	13022.90
11	1735/746	C=O stretching	4363.810	4708.97	3897.12	4222.31	4020.36	4117.51

Table 3 Unsaturated fatty acid content in adipose tissue samples from two pig breeds

Intensity (I) ratio of Raman signals	Livni			Duroc		
	Sacral	Axillary	Perirenal	Sacral	Axillary	Perirenal
I_{970}/I_{1297}	0.074597	0.084793	0.051299	0.087496	0.078953	0.056013
I_{970}/I_{1430}	0.047508	0.050224	0.040401	0.058050	0.053387	0.040915
I_{970}/I_{1735}	0.331676	0.326044	0.309944	0.419467	0.400079	0.298098
I_{1266}/I_{1297}	0.383491	0.471286	0.244688	0.394967	0.377758	0.289588
I_{1266}/I_{1430}	0.244227	0.279148	0.192707	0.262044	0.255435	0.211529
I_{1266}/I_{1735}	1.705081	1.812167	1.478399	1.893530	1.914217	1.541174
I_{1655}/I_{1297}	0.843839	1.082599	0.510407	0.823405	0.805197	0.594295
I_{1655}/I_{1430}	0.537401	0.641235	0.401977	0.546296	0.544463	0.434102
I_{1655}/I_{1735}	3.751882	4.162757	3.083867	3.947531	4.080182	3.162810
GeoMean	0.408874	0.461877	0.312392	0.448982	0.434953	0.334639

of Raman signals corresponding to unsaturated bonds to those of saturated or ester bonds (Table 3). The peaks at 970, 1266/1272, and 1655 cm^{-1} reflect the degree of unsaturation, while the signals at 1297/1301, 1430/1460, and 1735/1746 cm^{-1} correspond to saturated bonds or ester groups [35]. So we used nine intensity ratios to calculate, namely I_{970}/I_{1297} , I_{970}/I_{1430} , I_{970}/I_{1735} , I_{1266}/I_{1297} , I_{1266}/I_{1430} , I_{1266}/I_{1735} , I_{1655}/I_{1297} , I_{1655}/I_{1430} , and I_{1655}/I_{1735} . The relative amount of unsaturated fat in the sample was determined by calculating the geometric mean (GeoMean) of the ratios obtained.

Internal perirenal fat samples from both breeds showed a more intense peak of 1297/1301 cm^{-1} and less intense peaks of 970, 1266/1272, and 1655 cm^{-1} . The peak of 1430/1460 cm^{-1} showed no significant difference than subcutaneous fat samples. The geometric mean ratio of intensities was also minimal: 0.312392 for the perirenal Livni samples and 0.334639 for the perirenal Duroc samples. This may indicate a lower proportion of double-bonded fatty acids and a higher proportion of saturated fatty acids in internal fat. This result is in agreement with the work of Monziols *et al.* and Bee *et al.*, where it was shown that the degree of unsaturated fat deposition in pigs follows a negative gradient from outside to inside [16, 35]. The metabolic reasons for the preferential deposition of unsaturated fatty acids in subcutaneous fat are presumably related to low lipid metabolism. Internal fat exhibits greater *de novo* lipogenesis, with the result that feed-derived unsaturated fatty acids are diluted with more endogenous fatty acids than in subcutaneous fat.

The subcutaneous adipose tissue samples showed more intense peaks responsible for unsaturated bonds, while signals from saturated bonds did not show a uniform trend: 1297/1301 cm^{-1} was lower in all samples, 1430/1460 cm^{-1} with no significant difference, 1735/1746 cm^{-1} in the Livni breed samples was higher in subcutaneous fat (both locations), while in the Duroc breed it was higher in sacral fat and lower in axillary fat

than in perirenal fat. The axillary Livni samples were characterized by more intense signals from unsaturated bonds than the sacral Livni samples, 0.461877 and 0.408874 respectively, while the axillary Duroc fat, on the contrary, showed less intense signals than the sacral Duroc samples, 0.434953 and 0.448982 respectively.

In a comparative analysis of the spectra of the samples from Duroc and Livni pigs, sacral Duroc showed more intense signals from unsaturated bonds, whereas the signals from saturated bonds varied – 1297/1301 cm^{-1} higher and 1735/1746 cm^{-1} lower than in sacral Livni, while axillary Duroc was more saturated than axillary Livni.

CONCLUSION

Taken together, the findings confirm that in pigs, the adipose tissue of different locations differs in morphology, lipid content and composition. Our results show that there are differences in cellular structure between adipose tissue of different locations (subcutaneous and internal) of Duroc and Livni pigs, and that adipocyte hypertrophy contributes most to the greater deposition of subcutaneous fat in Livni pigs. Both breeds showed a biphasic distribution of adipocyte size at all loci, suggesting that adipocytes are in their growth and fat accumulation phase.

In the Raman spectroscopy analysis, the inner perirenal adipose tissue showed less intense signals from unsaturated bonds compared to the subcutaneous tissue irrespective of the pig breed. The axillary fat samples of the Livni breed were characterised by more intense peaks responsible for unsaturated bonds than the sacral fat. The sacral fat from the Duroc breed was more unsaturated than that of the Livni breed. Further studies of adipose tissue of different locations, including using Raman spectroscopy, are needed to establish the lipogenesis potential of these adipose tissues, especially in pigs with different grades of body fat.

In the future, pig adipose tissue will be studied in greater depth. Most of the published studies have been

conducted with the subcutaneous adipose tissue of pigs, but the morphology of inter- and intramuscular fat also needs study, as its content has a significant influence on the consumer characteristics of pork. So, a comparative study of adipocytes from other anatomical loci of pigs, their development and composition, as well as their impact on the quality and structural and functional properties of raw meat would be of interest.

CONTRIBUTION

The authors were equally involved in writing the manuscript and are equally responsible for plagiarism.

CONFLICT OF INTEREST

The authors state that there is no conflict of interest.

REFERENCES

1. Giuffra E, Kijas JMH, Amarger V, Carlborg O, Jeon J-T, Andersson L. The origin of the domestic pig: Independent domestication and subsequent introgression. *Genetics*. 2000;154(4):1785–1791. <https://doi.org/10.1093/genetics/154.4.1785>
2. Mikhailova OA. Tendencies of the world swine breeding development. *Bulletin of Agrarian Science*. 2018;70(1):36–45. (In Russ.). <https://doi.org/10.15217/issn2587-666X.2018.1.36>
3. Traspov A, Deng W, Kostyunina O, Ji J, Shatokhin K, Lugovoy S, *et al.* Population structure and genome characterization of local pig breeds in Russia, Belorussia, Kazakhstan and Ukraine. *Genetics Selection Evolution*. 2016;48(1). <https://doi.org/10.1186/s12711-016-0196-y>
4. Mikhailov NV, Baranikov AI, Svinarev IYu. Pig breeding. Pork production technology. Rostov-on-Don: Izdatel'stvo Yug; 2009. 417 p. (In Russ.).
5. Genetics made in Russia. The import of purebred breeding pigs has decreased by 3.7 times over five years [Internet]. [cited 2022 Aug 8]. Available from: <https://www.agroinvestor.ru/technologies/article/30688-genetika-made-in-russia>
6. Kharzinova VR, Zinovieva NA. The pattern of genetic diversity of different breeds of pigs based on microsatellite analysis. *Vavilov Journal of Genetics And Breeding*. 2020;24(7):747–754. (In Russ.). <https://doi.org/10.18699/VJ20.669>
7. Quan J, Gao C, Cai Y, Ge Q, Jiao T, Zhao S. Population genetics assessment model reveals priority protection of genetic resources in native pig breeds in China. *Global Ecology and Conservation*. 2020;21. <https://doi.org/10.1016/j.gecco.2019.e00829>
8. Gan M, Shen L, Fan Y, Guo Z, Liu B, Chen L, *et al.* Altitude adaptability and meat quality in Tibetan pigs: A reference for local pork processing and genetic improvement. *Animals*. 2019;9(12). <https://doi.org/10.3390/ani9121080>
9. Pugliese C, Sirtori F. Quality of meat and meat products produced from southern European pig breeds. *Meat Science*. 2012;90(3):511–518. <https://doi.org/10.1016/j.meatsci.2011.09.019>
10. Brossard L, Nieto R, Charneca R, Araujo JP, Pugliese C, Radović Č, *et al.* Modelling nutritional requirements of growing pigs from local breeds using InraPorc. *Animals*. 2019;9(4). <https://doi.org/10.3390/ani9040169>
11. Pavlova SV, Kozlova NA, Shchavlikova TN. Breeding base of pig breeding in Russia at the beginning of 2021. *Efficient Animal Husbandry*. 2021;171(5):28–31. (In Russ.).
12. Directions of productivity [Internet]. [cited 2022 August 08]. Available from: <https://www.websadovod.ru/pig/03.htm>
13. Bekenev VA, Arishin AA, Mager SN, Bolshakova IV, Tretyakova NL, Kashtanova EV, *et al.* Lipid profile of pig tissues contrasting in meat production. *Natural Products Journal*. 2021;11(1):108–118. <https://doi.org/10.2174/2210315509666191203124902>
14. Poklukar K, Čandek-Potokar M, Lukač NB, Tomažin U, Škrlep M. Lipid deposition and metabolism in local and modern pig breeds: A review. *Animals*. 2020;10(3). <https://doi.org/10.3390/ani10030424>
15. Monziols M, Bonneau M, Davenel A, Kouba M. Comparison of the lipid content and fatty acid composition of intermuscular and subcutaneous adipose tissues in pig carcasses. *Meat Science*. 2007;76(1):54–60. <https://doi.org/10.1016/j.meatsci.2006.10.013>
16. Sturm G, Susenbeth A, Ehrensverd U, Gmelin M, Loeffler K. The adaptation of the morphometric parameters of fat cell size for the purposes of animal science research. 2. Cellularity of subcutaneous adipose tissue of different swine breeds influenced by graduated feed levels and in relation to metabolic data and parameters of body fat degeneration. *Berliner und Munchener tierarztliche Wochenschrift*. 1990;103(4):112–117.
17. Chernukha IM, Fedulova LV, Kotenkova EA. White, beige and brown adipose tissue: structure, function, specific features and possibility formation and divergence in pigs. *Foods and Raw Materials*. 2022;10(1):10–18. <https://doi.org/10.21603/2308-4057-2022-1-10-18>
18. Hauser N, Mourot J, De Clercq L, Genart C, Remacle C. The cellularity of developing adipose tissues in Pietrain and Meishan pigs. *Reproduction. Nutrition. Development*. 1997;37(6):617–625. <https://doi.org/10.1051/rnd:19970601>

19. Nakajima I, Oe M, Ojima K, Muroya S, Shibata M, Chikuni K. Cellularity of developing subcutaneous adipose tissue in Landrace and Meishan pigs: Adipocyte size differences between two breeds. *Animal Science Journal*. 2011;82(1):144–149. <https://doi.org/10.1111/j.1740-0929.2010.00810.x>
20. Vincent A, Louveau I, Gondret F, Leuret B, Damon M. Mitochondrial function, fatty acid metabolism, and immune system are relevant features of pig adipose tissue development. *Physiological Genomics*. 2012;44(22):1116–1124. <https://doi.org/10.1152/physiolgenomics.00098.2012>
21. Ayuso D, González A, Peña F, Hernández-García FI, Izquierdo M. Effect of fattening period length on intramuscular and subcutaneous fatty acid profiles in Iberian pigs finished in the *Montanera* sustainable system. *Sustainability*. 2020;12(19). <https://doi.org/10.3390/su12197937>
22. Beattie JR, Bell SEJ, Borgaard C, Fearon A, Moss BW. Prediction of adipose tissue composition using Raman spectroscopy: Average properties and individual fatty acids. *Lipids*. 2006;41(3):287–294. <https://doi.org/10.1007/s11745-006-5099-1>
23. Romeis B. *Mikroskopische technik*. München: Urban u. Schwarzenberg; 1989. 697 p.
24. Velotto S, Vitale C, Crasto A. Muscle fibre types, fat deposition and fatty acid profile of Casertana versus Large White pig. *Animal Science Papers and Reports*. 2012;30(1):35–44.
25. Berhe DT, Eskildsen CE, Lametsch R, Hviid MS, van den Berg F, Engelsen SB. Prediction of total fatty acid parameters and individual fatty acids in pork backfat using Raman spectroscopy and chemometrics: Understanding the *cage of covariance* between highly correlated fat parameters. *Meat Science*. 2016;111:18–26. <https://doi.org/10.1016/j.meatsci.2015.08.009>
26. Louveau I, Perruchot M-H, Bonnet M, Gondret F. Invited review: Pre- and postnatal adipose tissue development in farm animals: From stem cells to adipocyte physiology. *Animal*. 2016;10(11):1839–1847. <https://doi.org/10.1017/S1751731116000872>
27. Zhao J, Tao C, Chen C, Wang Y, Liu T. Formation of thermogenic adipocytes: What we have learned from pigs. *Fundamental Research*. 2021;1(4):495–502. <https://doi.org/10.1016/j.fmre.2021.05.004>
28. Abbas O, Fernández Pierna JA, Codony R, von Holst C, Baeten V. Assessment of the discrimination of animal fat by FT-Raman spectroscopy. *Journal of Molecular Structure*. 2009;924–936:294–300. <https://doi.org/10.1016/j.molstruc.2009.01.027>
29. Saleem M, Amin A, Irfan M. Raman spectroscopy based characterization of cow, goat and buffalo fats. *Journal of Food Science and Technology*. 2021;58(1):234–243. <https://doi.org/10.1007/s13197-020-04535-x>
30. Czamara K, Majzner K, Pacia MZ, Kochan K, Kaczor A, Baranska M. Raman spectroscopy of lipids: A review. *Journal of Raman Spectroscopy*. 2014;46(1):4–20. <https://doi.org/10.1002/jrs.4607>
31. De Gelder J, De Gussem K, Vandenabeele P, Moens L. Reference database of Raman spectra of biological molecules. *Journal of Raman Spectroscopy*. 2007;38(9):1133–1147. <https://doi.org/10.1002/jrs.1734>
32. Afseth NK, Dankel K, Andersen PV, Difford GF, Horn SS, Sonesson A, et al. Raman and Near Infrared Spectroscopy for quantification of fatty acids in muscle tissue – A salmon case study. *Foods*. 2022;11(7). <https://doi.org/10.3390/foods11070962>
33. Determining pork fat quality as measured by three methods with an industry standard marketing plan for pigs fed 20% DDGS [Internet]. [cited 2022 August 08]. Available from: <https://porkcheckoff.org/wp-content/uploads/2021/02/12-045-WIEGAND-UofMO.pdf>
34. Lee J-Y, Park J-H, Mun H, Shim W-B, Lim S-H, Kim M-G. Quantitative analysis of lard in animal fat mixture using visible Raman spectroscopy. *Food Chemistry*. 2018;254:109–114. <https://doi.org/10.1016/j.foodchem.2018.01.185>
35. Bee G, Gebert S, Messikommer R. Effect of dietary energy supply and fat source on the fatty acid pattern of adipose and lean tissues and lipogenesis in the pig. *Journal of Animal Science*. 2002;80(6):1564–1574. <https://doi.org/10.2527/2002.8061564x>
36. Pchelkina VA, Chernukha IM, Fedulova LV, Ilyin NA. Raman spectroscopic techniques for meat analysis: A review. *Theory and Practice of Meat Processing*. 2022;7(2):97–111. <https://doi.org/10.21323/2414-438X-2022-7-2-97-111>

ORCID IDs

Viktoriya A. Pchelkina <https://orcid.org/0000-0001-8923-8661>
Irina M. Chernukha <https://orcid.org/0000-0003-4298-0927>
Marina A. Nikitina <https://orcid.org/0000-0002-8313-4105>
Nikolai A. Ilin <https://orcid.org/0000-0002-7980-3193>